

# Spectropolarimetric Study on Circumstellar Structure of Microquasar LS I +61° 303

Osamu NAGAE<sup>1,2</sup> Koji S. KAWABATA<sup>2,3</sup> Yasushi FUKAZAWA<sup>1</sup>  
Takuya YAMASHITA<sup>2,3</sup> Takashi OHSUGI<sup>1,3</sup> Makoto UEMURA<sup>3</sup> Shingo CHIYONOBU<sup>1,2</sup>  
Mizuki ISOGAI<sup>2,4</sup> Toshinari CHO<sup>2,4</sup>  
Masaaki SUZUKI<sup>2,4</sup> Akira OKAZAKI<sup>5</sup> Kiichi OKITA<sup>6</sup> and Kenshi YANAGISAWA<sup>6</sup>

<sup>1</sup>*Department of Physical Science, School of Science, Hiroshima University,  
1-3-1 Kagamiyama, Higashi-hiroshima, Hiroshima 739-8526, Japan*  
*nagae@hirax7.hepl.hiroshima-u.ac.jp*  
*fukazawa@hirax7.hepl.hiroshima-u.ac.jp*  
*ohsugi@hirax7.hepl.hiroshima-u.ac.jp*  
*chiyo@hirax7.hepl.hiroshima-u.ac.jp*

<sup>2</sup>*Visiting Astronomer, Okayama Astrophysical Observatory,  
National Astronomical Observatory of Japan (NAOJ)*

<sup>3</sup>*Hiroshima Astrophysical Science Center, Hiroshima University,  
1-3-1 Kagamiyama, Higashi-hiroshima, Hiroshima 739-8526, Japan*  
*kawabtkj@hiroshima-u.ac.jp*  
*yamashitak@hiroshima-u.ac.jp*  
*uemuram@hiroshima-u.ac.jp*

<sup>4</sup>*Astronomical Institute, Graduate School of Science, Tohoku University,  
Aoba, Aramaki, Aoba-ku, Sendai, Miyagi 980-8578, Japan*  
*iso@astr.tohoku.ac.jp*  
*cho@astr.tohoku.ac.jp*  
*szk\_masa@astr.tohoku.ac.jp*

<sup>5</sup>*Department of Science Education, Gunma University,  
4-2 Aramaki, Maebashi Gunma 371-8510, Japan*  
*okazaki@edu.gunma-u.ac.jp*

<sup>6</sup>*Okayama Astrophysical Observatory, NAOJ,  
3037-5 Honjo, Kamogata, Asakuchi 719-0232, Japan*  
*okita@oao.nao.ac.jp*  
*yanagi@oao.nao.ac.jp*

(Received 2000 December 31; accepted 2001 January 1)

## Abstract

We present optical linear spectropolarimetry of the microquasar LS I +61° 303.

The continuum emission is mildly polarized (up to 1.3 %) and shows almost no temporal change. We find a distinct change of polarization across the H $\alpha$  emission line, indicating the existence of polarization component intrinsic to the microquasar. We estimate the interstellar polarization (ISP) component from polarization of the H $\alpha$  line and derive the intrinsic polarization component. The wavelength dependence of the intrinsic component is well explained by Thomson scattering in equatorial disk of the Be-type mass donor. The position angle (PA) of the intrinsic polarization  $\sim 25^\circ$  represents the rotational axis of the Be disk. This PA is nearly perpendicular to the PA of the radio jet found during quiescent phases. Assuming an orthogonal disk-jet geometry around the compact star, the rotational axis of the accretion disk is almost perpendicular to that of the Be disk. Moreover, according to the orbital parameters of the microquasar, the compact star is likely to get across the Be disk around their periastron passage. We discuss the peculiar circumstellar structure of this microquasar inferred from our observation and possible connection with its high-energy activities.

## 1. Introduction

A microquasar is an X-ray binary system displaying relativistic radio jets (see review of Ribó 2005 and references therein). It consists of a compact star (neutron star or stellar-mass blackhole) and a mass donor star. About 20 microquasars have been identified in our galaxy to date (Paredes 2005). They are likely to be scaled-down version of radio-loud active galactic nuclei because of their morphological and physical similarities (relativistic jet ejection and blackhole engine). A microquasar provides an excellent laboratory for study of mass accretion and ejection phenomena in a strong gravitational field on human timescales. Their spectra extend from radio to  $\gamma$ -rays (e.g. Mirabel & Rodriguez 1999). Optical emission from microquasars are usually considered to be either thermal emission emerged from outer part of the accretion disk around the compact star (low-mass donor case) or stellar light of the mass donor (high-mass case). However, recent observations suggest that some microquasars show synchrotron emission even at optical wavelengths in outburst phases (Kanbach et al. 2001; Uemura et al. 2004).

Optical polarimetric observation can be unique to probe microquasar systems, since we can obtain information on jets (e.g., geometry, magnetic field, electron energy) from synchrotron emission or on geometrical properties of the binary system from the light scattered by circumstellar matter (accretion disk and/or stellar wind) in a scale not being accessible by contemporary imaging techniques. Several optical polarimetric studies of microquasars have been reported for, e.g., LS 5039 (Combi et al. 2004), GRO J1655-40 (Scaltriti et al. 1997; Gliozzi et al. 1998), and SS 433 (Efimov et al. 1984) so far. They revealed the presence of intrinsic polarization. However, all of these studies employed broad-band filters which can

not reveal how the polarization correlates with the spectral features. Spectropolarimetry permits separation of the line and continuum components, providing a more accurate way to find intrinsic and interstellar components of the observed polarization.

We made optical spectropolarimetric observations of the microquasar LS I +61° 303. This is one of Be/X-ray binary systems, having a large eccentricity of  $e = 0.72 \pm 0.15$  (Casares et al. 2005). This object is an optical counterpart of the variable radio source GT 0236+610, which was discovered within  $1\sigma$  error circle of the  $\gamma$ -ray source 2CG 135+01 = 3EG J0241+6103 (Gregory & Taylor 1978). This source exhibits radio outbursts every 26.5 days (Taylor & Gregory 1982). Nearly identical periodicity has been found in X-rays ( $26.42 \pm 0.05$  days; Paredes et al. 1997). They are consistent with the orbital period determined by optical and infrared observations (Hutchings & Crampton 1981; Paredes et al. 1994; Gregory 2002). Similar periodicity has also been suggested in  $\gamma$ -rays ( $27.4 \pm 7.2$  days; Massi 2004b), which supports the physical connection of LS I +61° 303 with 3EG J0241+6103. Recently, Albert et al. (2006) found very high energy  $\gamma$ -ray emission (above 100 GeV) showing a possible periodicity. Based on the *IUE* ultraviolet and ground-based spectroscopy, the mass donor of LS I +61° 303 is classified as a B0Ve star (Hutchings & Crampton 1981). Long monitoring of radio flux (Gregory et al. 1999) and H $\alpha$  line emissions (Zamanov et al. 1999) indicated that the mass-loss rate of the Be star has a period of about 4.6 yr. Radio interferometric observations found that the axis of radio jet rapidly rotated in the projected sky plane (Massi et al. 2004a), giving an S-shaped morphology like SS 433 (Hjellming & Johnston 1988) and a ‘micro-blazer’ model (Kaufman Bernadó, Romero, Mirabel 2002; Romero, Kaufman Bernadó, & Mirabel 2002) is proposed for this binary.

In this paper, we examine a circumstellar structure of LS I +61° 303 with our new spectropolarimetric data. We describe the observations and data reduction in §2, and show the results in §3. We discuss the circumstellar structure of LS I +61° 303 in §4. Then, we summarize our study in §5.

## 2. Observations and Data Reduction

The observations were performed on two nights in 2005 January (epoch 1) and on six nights in 2005 October and November (epoch 2) with a low-resolution spectropolarimeter, HBS (Kawabata et al. 1999), attached to the 1.88m telescope at Okayama Astrophysical Observatory, National Astronomical Observatory of Japan (NAOJ). The log of the observations is shown in Table 1. HBS has a superachromatic half-wave plate and a quartz Wollaston prism, giving a capability of measuring linear polarization in a wide range of optical region (4000-9000 Å). We employed a SITe  $512 \times 512 \times 24 \mu\text{m}$  CCD camera (MicroLuminetics, Inc.) with in epoch 1 and a Marconi  $2048 \times 512 \times 13.5 \mu\text{m}$  CCD camera (Andor Tech, Inc.) in epoch 2. We used a slit of 0.2mm width, yielding a wavelength resolution of  $\sim 60 \text{ \AA}$ . A unit of the observing sequence consists of successive integrations at 0°, 22.5°, 45° and 67.5° position angles of the

half-wave plate.

Data reduction was performed using a standard software developed for HBS observations, HBSRED (Kawabata et al. 1999). For polarimetric calibration, we used data of polarized and unpolarized standard stars (Wolff, Nordsieck, & Nook 1996), obtained with or without a fully-polarizing, Glan-Taylor prism. Polarimetric accuracy estimated from peak-to-peak variation of unpolarized standard star data was  $\sim 0.05\%$  over the observed wavelength range. The flux was calibrated using data of spectrophotometric standard stars (Taylor 1984).

### 3. Results

#### 3.1. Overall polarization properties

Figure 1 shows observed polarization spectra (degree of polarization  $P_{\text{obs}}$  and its position angle  $\theta_{\text{obs}}$ ) on 2005 Oct 27 and Nov 8. The continuum emission exhibits rather smooth wavelength dependence over the optical region. The nightly-averaged V-band polarization data are shown in Table 1, which indicates that there was no significant time variation in the continuum polarization over the period of our observations. Figure 2 shows an enlarged plot around the  $H\alpha$  emission line. It indicates an apparent change of polarization across the  $H\alpha$  line, suggesting the existence of a polarization component intrinsic to LS I +61° 303. We discuss it in §3.3.

#### 3.2. Equivalent width of $H\alpha$ emission line

$H\alpha$  emission of a Be star is thought to originate mostly from equatorial disk around the star (e.g., Quirrenbach et al. 1997). Paredes et al. (1994) and Zamanov et al. (1999) revealed that equivalent width (EW) of  $H\alpha$  line in LS I +61° 303 changes with a possible period of  $\sim 4.6$  yr. This is considered to reflect the variation of mass-loss rate of the Be star. Figure 3 displays the mass-loss phase dependency of the EWs derived from our data together with those from literature, which shows that EWs of our data were commonly at low level compared with the past observations. It suggests that the disk of the Be star has not developed very much and the  $\sim 4.6$  yr periodicity is unclear during our observation. According to AAVSO<sup>1</sup> database any significant brightness change was not reported during the period of our observation. These facts imply that the binary system was in a quiescent phase in the optical light.

#### 3.3. Interstellar polarization

Observed polarization is generally expressed as a vectorial sum of intrinsic polarization and interstellar polarization (ISP), i.e.,

$$q_{\text{obs}}(\lambda) = q_{\text{int}}(\lambda) + P_{\text{ISP}}(\lambda) \cos 2\theta_{\text{ISP}}, \quad u_{\text{obs}}(\lambda) = u_{\text{int}}(\lambda) + P_{\text{ISP}}(\lambda) \sin 2\theta_{\text{ISP}}, \quad (1)$$

where  $(q_{\text{obs}}, u_{\text{obs}})$  and  $(q_{\text{int}}, u_{\text{int}})$  are Stokes parameters of the observed polarization and the intrinsic polarization, respectively.  $P_{\text{ISP}}$  and  $\theta_{\text{ISP}}$  are degree of the ISP and its position angle,

<sup>1</sup> <http://www.aavso.org/>

respectively. ISP is produced by dichroic absorption by magnetically-aligned aspherical dust grains existing between the object and the earth. To derive the intrinsic polarization, it is essentially important to know the ISP component accurately. The degree of ISP is well expressed by a smooth function of wavelength in optical region as,

$$P_{\text{ISP}}(\lambda) = P_{\text{max}} \exp(-K \ln^2 \frac{\lambda_{\text{max}}}{\lambda}), \quad (2)$$

where  $P_{\text{max}}$  is the peak polarization degree of the ISP at wavelength  $\lambda_{\text{max}}$  (Serkowski et al. 1975). Upper-limit of  $P_{\text{max}}$  is practically fixed by color excess,  $E_{B-V}$ , as

$$P_{\text{max}} \leq 9.0 \times E_{B-V} \quad (3)$$

(Serkowski et al. 1975). Paredes & Figueras (1986) derived  $E_{B-V} = 1.13$  for LS I +61° 303, which leads to  $P_{\text{max}} \leq 10.2\%$  and a median value of  $P_{\text{max}} \sim 5.1\%$  (Serkowski et al. 1975). The observed polarization degree  $P_{\text{obs},V} \sim 1.3\%$  (See Table 1) is much smaller than the expected degree of polarization. It suggests that the ISP is partly canceled out by non-zero intrinsic polarization of which the PA is nearly orthogonal to that of the ISP. To confirm it, we fit the Serkowski function (Eqn. 2) to the observed polarization data and derived the ISP parameters. Figure 4 shows the obtained  $K$  and  $\lambda_{\text{max}}$  values, together with the  $K$ - $\lambda_{\text{max}}$  relation derived by Whittet et al. (1992),

$$K = (1.66 \pm 0.09) \lambda_{\text{max}}(\mu\text{m}) + 0.01 \pm 0.05 \quad (4)$$

This figure shows that most of our data points detach from the linear  $K$ - $\lambda_{\text{max}}$  relation, which is also consistent with the idea that the observed polarization has a substantial intrinsic component.

To evaluate the ISP component, we used the change of polarization across the H $\alpha$  emission line. Line emission generally emerges from optically-thin regions and is subject to less scattering than continuum emission. This leads to a lower polarization level in the line emission than in the continuum emission. In the case of LS I +61° 303, the line emission is thought to arise from ionized gas of the Be disk. Without a few exceptions, we can consider that the line emission in Be stars should show little or no polarization (e.g. Poeckert 1975; Poeckert & Marlborough 1977; McLean & Clarke 1979; Quirrenbach et al. 1997). Therefore, we assume that the polarization of the line component practically represents the ISP. To subtract the continuum component from the polarization at H $\alpha$  emission line (denoted by suffix ‘em’), we used its neighboring continuum polarization on both sides of the line (‘con1’ and ‘con2’). We derive Stokes parameters  $I, Q, U$  of the line emission as

$$I_{\text{H}\alpha} = \Delta\lambda_{\text{em}} \left( \frac{I_{\text{em}}}{\Delta\lambda_{\text{em}}} - \frac{I_{\text{con1}} + I_{\text{con2}}}{\Delta\lambda_{\text{con1}} + \Delta\lambda_{\text{con2}}} \right), \quad (5)$$

$$Q_{\text{H}\alpha} = \Delta\lambda_{\text{em}} \left( \frac{q_{\text{em}} \times I_{\text{em}}}{\Delta\lambda_{\text{em}}} - \frac{q_{\text{con1}} \times I_{\text{con1}} + q_{\text{con2}} \times I_{\text{con2}}}{\Delta\lambda_{\text{con1}} + \Delta\lambda_{\text{con2}}} \right), \quad (6)$$

$$U_{\text{H}\alpha} = \Delta\lambda_{\text{em}} \left( \frac{u_{\text{em}} \times I_{\text{em}}}{\Delta\lambda_{\text{em}}} - \frac{u_{\text{con1}} \times I_{\text{con1}} + u_{\text{con2}} \times I_{\text{con2}}}{\Delta\lambda_{\text{con1}} + \Delta\lambda_{\text{con2}}} \right), \quad (7)$$

where  $\Delta\lambda$  is the band width of each component (em, con1 and con2). We set all  $\Delta\lambda$  to be 150 Å and the central wavelength of the H $\alpha$  emission band to be 6563 Å. There is no significant line component in those bands except for the H $\alpha$  line. We calculate the polarization degree and PA as

$$P_{\text{H}\alpha} = \frac{\sqrt{Q_{\text{H}\alpha}^2 + U_{\text{H}\alpha}^2}}{I_{\text{H}\alpha}}, \quad (8)$$

$$\theta_{\text{H}\alpha} = \frac{1}{2} \arctan\left(\frac{U_{\text{H}\alpha}}{Q_{\text{H}\alpha}}\right). \quad (9)$$

The derived H $\alpha$  polarization is shown in Table 1. Weighted-mean and standard deviation of all the eight nights data are  $P_{\text{H}\alpha} = 2.16 \pm 0.20\%$  and  $\theta_{\text{H}\alpha} = 126.4^\circ \pm 4.5^\circ$ , respectively. These values are comparable to the polarization of the field stars within 3 degree ( $4.3 \pm 1.1\%$ ,  $112 \pm 7^\circ$ ; Heiles 2000). Since PA of the ISP is almost constant with wavelength, we consider that  $\theta_{\text{H}\alpha}$  represents  $\theta_{\text{ISP}}$ . To derive the spectrum of the intrinsically polarized component, we should know the wavelength dependence of degree of the ISP, further. Once  $\lambda_{\text{max}}$  is fixed, the remaining ISP parameters,  $K$  and  $P_{\text{max}}$ , are calculated from Equations (2), (4) and the derived  $P_{\text{H}\alpha}$ . Serkowski et al. (1975) indicated that ISP has a peak polarization at  $\sim 5400 \pm 600$  Å in the case of  $P_{\text{max}}/E_{B-V} < 3$ . We thus assume that  $\lambda_{\text{max}}$  is 5000 Å, 5500 Å, or 6000 Å, and calculate the intrinsic polarization.

### 3.4. Origin of intrinsic polarization

Figure 5 shows the spectra of the intrinsic polarization for different  $\lambda_{\text{max}}$ . The wavelength dependence of the intrinsic polarization is closely similar to those of typical Be stars, e.g.  $\zeta$  Tau (Wood et al. 1997). The polarization of Be stars is explained by the result of Thomson scattering in their equatorial disks. If there is only one polarizing component (e.g. a single disk), the PA of the intrinsic polarization  $\theta_{\text{int}}$  should be constant against wavelength. This assumption is reasonable for most Be stars. The derived  $\theta_{\text{int}}$  becomes rather flat for  $\lambda_{\text{max}}$ , suggesting that the assumptions of the range of  $\lambda_{\text{max}}$  and the Be star-origin polarization are self-consistent. Therefore, we conclude that the origin of the intrinsic polarization is predominantly Thomson scattering in the Be star.

## 4. Discussion

### 4.1. Topology of the Be equatorial disk and orbital plane

Neither  $\theta_{\text{int}}$  nor the EW of the H $\alpha$  line do show temporal variation, which suggests that the Be equatorial disk is nearly stable during the period of our observation.  $\theta_{\text{int}} \sim 25^\circ$  implies that the PA of the Be disk is  $\sim 115^\circ$  (PA of polarization is perpendicular to the scattering plane defined by the light source, the scatterer, and the observer) and the rotational axis of the Be star is at PA  $\sim 25^\circ$ . As noted in §1, radio jets have been found in LS I +61° 303. Table 2 shows PA's of the radio jets in literature. The directions of the jets seem to be biased around

PA $\sim$ 120 $^\circ$  during quiescent phases. If we can assume that the radio jets are perpendicular to the plane of the accretion disk around the compact object, the PA of the semi-major axis of the accretion disk on the projected sky would be  $\sim$ 30 $^\circ$ . No X-ray pulsation (e.g., Goldoni & Mereghetti 1995) suggests that the compact star is not strongly-magnetized and such an orthogonal disk-jet geometry can be assumed. We also consider that the plane of the accretion disk represents the orbital plane of the binary system. Thus, we propose a geometrical model in which the rotational axis of the Be star is almost perpendicular to the orbital plane as shown in Figure 6. Considering an evolution of a typical binary system whose member stars were born in a same molecular cloud, our geometrical model seems to be quite peculiar. However, a similar geometry has been reported in another Be/X-ray binary system, PSR B 1259-63 (Wex et al. 1998 and Wang et al. 2004). They suggested that the Be equatorial disk is considerably tilted with respect to the orbital plane, and Chernyakova et al. (2006) suggested that the tilt angle is about 70 $^\circ$ . These studies may support our picture for LS I +61 $^\circ$  303. We will discuss possible origin of this peculiar topology in §4.4.

#### 4.2. Inclination of Be equatorial disk

Considering a light scattering model derived by Cassinelli, Nordsieck & Murison (1987), we can estimate the inclination angle  $i'$  of the rotational axis of the Be disk against the line of sight. The expected degree of the polarization is given by

$$P = -\frac{3\sigma_T \sin^2 i'}{16} \int_r \int_\mu (1 - 3\mu^2) D(r) n_e(r, \mu) d\mu dr \quad (10)$$

where  $P$  is a degree of polarization,  $\sigma_T$  is the Thomson scattering cross-section,  $\mu$  is  $\cos \theta$  and  $\theta$  is a polar angle against the rotational axis of the Be star.  $D(r) = (1 - R_*^2/r^2)^{1/2}$  is the finite disk depolarization factor.  $D(r)$  rises from 0 to 1 as  $r$  changes from  $R_*$  (stellar surface) to  $+\infty$ .  $n_e$  is an electron number density of the ionized gas. We assume that the ionized gases exist in a disk form as

$$n_e(r, \mu) = \begin{cases} n_e(r) = \frac{\dot{M}_w / (1 - \mu_{hoa}^2)}{4\pi v(r) r^2} \times \frac{1}{m_H} & (90^\circ - \theta_{hoa} \leq \theta \leq 90^\circ + \theta_{hoa}) \\ 0 & (\theta < 90^\circ - \theta_{hoa} \text{ and } 90^\circ + \theta_{hoa} < \theta) \end{cases} \quad (11)$$

where  $\dot{M}_w$  is a wind mass loss rate,  $\mu_{hoa} = \cos \theta_{hoa}$ ,  $\theta_{hoa}$  is a half opening angle of the equatorial disk,  $m_H$  is a mass of hydrogen atom, and  $v(r) = v_0 + (v_\infty - v_0)(1 - R_*/r^2)$  is a wind velocity of Be star (Castor & Lamers 1979). We set the initial velocity to  $v_0 \sim 5 \text{ km s}^{-1}$  and the terminal velocity to  $v_\infty \sim 200 \text{ km s}^{-1}$  (Waters et al. 1988). Adopting  $P \sim 1.5\%$ , the intrinsic polarization at  $\sim 4000 \text{ \AA}$  where the effect of the unpolarized bound-free emission of hydrogen is nearly negligible,  $\theta_{hoa} \sim 7\text{-}15^\circ$  (Waters et al. 1988; Martí & Paredes 1995), and  $\dot{M}_w \sim (0.4\text{-}4) \times 10^{-7} M_\odot/\text{yr}$  (Martí & Paredes 1995), we can get  $i' \sim 20\text{-}50^\circ$  from Equations (10) and (11). Ultraviolet spectroscopy indicates that the rotational velocity of the Be star is  $V \sin i' = 360 \pm 25 \text{ km s}^{-1}$  (Hutchings & Crampton 1981). By assuming that the maximum rotational

velocity of Be stars is  $V_{\max} = 630 \times 0.9 = 570 \text{ km s}^{-1}$  (Hutchings et al. 1979), Massi et al. (2001) suggested the lower limit for the inclination of the equatorial disk as  $\sim 38^\circ$ . Combining our result, we suggest that the inclination angle of the Be disk is  $i' \simeq 38\text{-}50^\circ$ .

#### 4.3. Geometrical model of LS I +61° 303

Orbital parameters of LS I +61° 303 have been derived from optical spectroscopy as orbital eccentricity  $e = 0.72 \pm 0.15$  and  $a \sin i = 8.2 \pm 2.9 R_\odot$  where  $a$  is the length of major axis of the orbit and  $i$  is the inclination angle between the orbital axis and the line of sight (Casares et al. 2005). From  $e$  and  $a \sin i$ , we can estimate the distance of the compact star from the Be star at their periastron passage as  $d_{\text{peri}} = a(1 - e)$ . Considering the range of  $\pm 1\sigma$  error in both  $e$  and  $a \sin i$ , we calculate  $d_{\text{peri}}$  for  $i = 0^\circ - 90^\circ$  as shown in Figure 7. This figure suggests that the separation at the periastron passage is less than  $\sim 30 R_\odot$  in most cases for  $i \gtrsim 10^\circ$ . If the outer radius of the Be equatorial disk is  $\sim 3R_* = 30 R_\odot$  (Waters et al. 1988), the compact star is likely to get across the Be equatorial disk, nearly perpendicularly as discussed in §4.1 For larger  $i$  ( $\gtrsim 30^\circ$ ), the compact star would pass through the inside of the Be stellar surface. In this case, a drastic dip of high energy emission would be observed around the periastron passage ( $\Phi \simeq 0.23$ ). However, such a phenomenon has not been reported (e.g. Paredes et al. 1999; Harrison et al. 2000; Massi 2004b), and we can reject the case of  $d_{\text{peri}} \lesssim R_*$  and suggest  $i \lesssim 30^\circ$ . This condition is comparable to the condition ( $i \lesssim 28 \pm 11^\circ$ ), derived under the assumption that the compact star is not eclipsed by the Be star (radius  $\simeq 10 R_\odot$ ) even at the conjunction ( $\Phi = 0.16$ , Casares et al. 2005). When the compact star gets across the Be equatorial disk, the accretion disk around the compact star may obtain angular momentum which is different from that of the spherical wind of the Be star. Using Bondi-Hoyle accretion model<sup>2</sup> (Bondi & Hoyle 1944) together with mass-loss model in Waters et al. (1988) ( $v_\infty \sim 2000 \text{ km s}^{-1}$ , and  $\dot{M}_w \sim 10^{-8} M_\odot \text{ yr}^{-1}$  for the spherical wind, and  $v_\infty \sim 200 \text{ km s}^{-1}$  and  $\dot{M}_w \sim 10^{-7} M_\odot \text{ yr}^{-1}$  for the equatorial wind), and a disk geometry model same as §4.1, we estimate the mass accretion rate on to the compact star. The accretion rate during the passage through the equatorial disk at  $\sim 3R_*$  ( $\dot{M}_{w,\text{disk}}$ ) is  $\sim 8 \times 10^{-7} M_\odot \text{ yr}^{-1}$  and the spherical wind at the same passage ( $\dot{M}_{w,\text{sw}}$ ) is  $\sim 7 \times 10^{-13} M_\odot \text{ yr}^{-1}$ . Thus,  $\dot{M}_{w,\text{disk}}$  is about 6 order higher than  $\dot{M}_{w,\text{sw}}$ . The derived value of  $\dot{M}_{w,\text{disk}}$  is about 40 times higher than the Eddington accretion rate of a typical neutron star, and it is unlikely that such a high rate accretion actually occurs in the case of a neutron star primary. But, the large difference in  $\dot{M}_w$  would lead to sudden changes of accretion properties and the resultant mass ejection. Such an impulsive change gives a hint on the formation and the precession of the radio jet. However, the launch of the precessing jet occurred at  $\Phi \sim 0.7$ , largely apart from the periastron  $\Phi \simeq 0.23$ . It has been known that both the radio and X-ray emission modulate with the orbital phase (Harrison et al. 2000 and references therein) and that there is a significant offset between their peaks ( $\Delta\Phi \sim 0.4\text{-}0.5$ ). The

<sup>2</sup> Assuming Kepler rotation, we found the rotational velocity of Be equatorial disk ( $250 \text{ km s}^{-1}$ ).



radio peaks are distributed over a wide phase interval of about 0.45-0.95 (Paredes et al. 1990). Harrison et al. (2000) suggests that X-ray emission is produced by inverse Compton scattering of stellar photons by relativistic electrons produced at the shock interaction of the relativistic between jet and Be star wind near the periastron, and the synchrotron radio emission would then arise from the expansion of the plasma around the apoastron passage. Along with this scenario, the launch of the precessing jet at  $\Phi \sim 0.7$  does not seem to be directly connected with the activities inferred from orbital modulations of X-ray and radio fluxes. More speculatively, we suggest that the time lag between the periastron passage and the jet launch represent the timescale of the mass accretion through the accretion disk. To examine the mechanism of the jet formation we should gain more observational information, e.g., more precise X-ray and  $\gamma$ -ray monitoring around  $\Phi \sim 0.7$ .

#### 4.4. *On the origin of peculiar topology*

Mirabel, Rodrigues & Liu (2004) suggested that the past supernova explosion in LS I +61° 303 (which produced the compact object) should be asymmetric to kick the compact object up to the highly eccentric ( $e \simeq 0.7$ ) orbit. The asymmetric explosion would also give a proper motion to the binary,  $\mu \sim 1.55 \text{ mas yr}^{-1}$  ( $27 \text{ km s}^{-1}$ ) and its PA  $\sim 141^\circ$ , escaping from its possible birth place IC 1805 (Lestrade et al. 1999; Mirabel, Rodrigues & Liu 2004). X-ray observations of several young pulsars have provided evidence for approximate alignment between the pulsar proper motion and its spin axis (Lai et al. 2001; Romani & Ng 2003). This may lead the spin axis of PA  $\sim 141^\circ$  for the compact object of LS I +61° 303, if it is a neutron star. However, it is unclear that we can adopt the spin-kick alignment mechanism to this binary because the proper motion is much less than the typical kick velocity of several hundred  $\text{km s}^{-1}$ . The asymmetric explosion might have had effects selectively on the binary orbit only.

## 5. Summary

We performed optical spectropolarimetry of the microquasar LS I +61° 303. We precisely estimated the ISP component from the H $\alpha$  line emission and derived the intrinsic polarization. Our main results can be summarized as follows: (1) The wavelength dependence of the intrinsic polarization is explained by Thomson scattering in the equatorial disk of Be star. (2) We found that the PA of the semi-major axis of the Be disk on the projected sky is almost parallel to the PA of the radio jet observed in quiescent phase. If we assume that the radio jet is perpendicular to the accretion disk of compact star, the Be disk is approximately orthogonal to that of the accretion disk. (3) The inclination of the Be disk is  $i' \simeq 38\text{-}50^\circ$ . (4) The compact star is likely to get across the Be disk around the periastron passage suggesting a drastic change of mass accretion rate ( $\dot{M}_{w,\text{disk}}/\dot{M}_{w,\text{sw}} \sim 10^6$ ). Speculatively, we suggest that this might be related with the precession of the radio jet axis. LS I +61° 303 is one of the the ideal laboratories to research

the peculiar activity of microquasars. Future phase-resolved multi-wavelength monitoring is required to examine the jet launching.

We are grateful to the staff members at Okayama Astrophysical Observatory of NAOJ for their kind support. We also thank to Kozo Sadakane and Yuji Norimoto for the opportunity of employing the Andor CCD camera. This work was partly supported by a Grant-in-Aid from the Ministry of Education, Culture, Sports, Science, and Technology of Japan (17684004). We thank an anonymous referee for helpful comments.

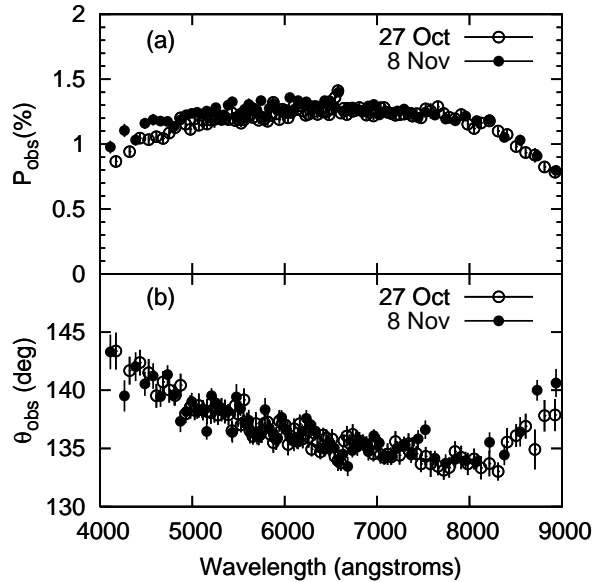


**Fig. 1.** Polarization spectra of LS I +61° 303 on 2005 Oct 27 and Nov 8. Upper panel (a) shows degree of polarization  $P_{\text{obs}}$ , and the lower one (b) shows its position angle  $\theta_{\text{obs}}$ . The polarimetric data are binned to a constant photon noise of 0.02%, and the observational error( $1\sigma$ ) in each bin is shown by a vertical error bar.

## References

- Albert, J. , et al. 2006, Sci, 312, 1771  
 Bessell, M. S. 1990, PASP, 102, 1181  
 Bondi, H., & Hoyle, F. 1944, MNRAS, 104, 273  
 Casares, J., Ribas, I., Paredes, J.M., Martí, J., & Allende Prieto, C. 2005, MNRAS, 360, 1105  
 Cassinelli, J. P., Nordsieck, K.H., & Murison, M.A. 1987, ApJ, 317, 290  
 Castor, J.I., & Lamers, H.J.G.L.M. 1979, ApJS, 39, 481  
 Chernyakova, M., Neronov, A., Lutovinov, A., Rodriguez, J., & Johnston, S. 2006, MNRAS, 367, 1201  
 Combi, J.A., Cellone, S.A., Martí, J., Ribo, M., Mirabel, I.F., & Casares, J. 2004, A&A, 427, 959  
 Efimov, Iu. S., Shakkovskoi, N. M., & Piirola, V. 1984, A&A, 138, 62  
 Fender, R. P., Bell Burnel, S. J., & Waltman, E. B. 1997, VA, 41, 3  
 Gliozzi, M., Bodo, G., Ghisellini, G., Scaltriti, F., & Trussoni, R. 1998 , A&A, 337, L39  
 Goldni, P., & Mereghetti, S. 1995, A&A, 299, 751  
 Gregory, P.C., & Taylor, A.R. 1978, Nature, 272, 704  
 Gregory, P. C., Peracaula, M., & Taylor, A. R. 1999, ApJ, 520, 376  
 Gregory, P.C. 2002, ApJ, 575, 427  
 Harrison, F. A., Ray, P. S., Leahy, D. A., Waltman, E. B., & Pooley, G. G. 2000, ApJ, 528, 454  
 Heiles, C. 2000, AJ, 119, 923  
 Hjellming, R.M., & Johnston, K.J. 1988, ApJ, 328, 600  
 Hutchings, J. B., Nemeč, J. M., & Cassidy, J. 1979, PASP, 91, 313  
 Hutchings, J.B., & Crampton, D. 1981, PASP, 93, 486

**Table 1.** Observation log

UT	JD	$\Phi^a$	Exposure <sup>b</sup> (s)	EW of H $\alpha$ ( $\text{\AA}$ )	$P_{\text{obs}}^c$ (%)	$\theta_{\text{obs}}^c$ ( $^\circ$ )	$P_{\text{H}\alpha}^d$ (%)	$\theta_{\text{H}\alpha}^d$ ( $^\circ$ )
2005 Jan 21.5	2453392.0	0.37	300 $\times$ 36	7.98 $\pm$ 0.09	1.22 $\pm$ 0.03	138.8 $\pm$ 0.7	2.21 $\pm$ 0.93	129.3 $\pm$ 18.6
2005 Jan 28.5	2453399.0	0.63	300 $\times$ 44	9.89 $\pm$ 0.15	1.31 $\pm$ 0.03	137.8 $\pm$ 0.6	1.85 $\pm$ 0.51	127.6 $\pm$ 14.7
2005 Oct 27.6	2453671.1	0.90	300 $\times$ 64	9.61 $\pm$ 0.09	1.20 $\pm$ 0.02	137.2 $\pm$ 0.5	2.63 $\pm$ 0.36	125.6 $\pm$ 7.00
2005 Oct 30.7	2453674.2	0.94	300 $\times$ 68	9.15 $\pm$ 0.11	1.26 $\pm$ 0.02	138.2 $\pm$ 0.5	2.38 $\pm$ 0.47	123.5 $\pm$ 10.1
2005 Nov 6.7	2453681.2	0.28	300 $\times$ 40	9.30 $\pm$ 0.11	1.30 $\pm$ 0.03	137.1 $\pm$ 0.6	2.53 $\pm$ 1.01	130.9 $\pm$ 20.1
2005 Nov 7.7	2453682.2	0.32	300 $\times$ 68	10.10 $\pm$ 0.11	1.31 $\pm$ 0.04	137.9 $\pm$ 0.8	1.74 $\pm$ 0.57	128.0 $\pm$ 17.0
2005 Nov 8.6	2453683.1	0.35	300 $\times$ 56	10.11 $\pm$ 0.11	1.27 $\pm$ 0.02	137.8 $\pm$ 0.4	1.67 $\pm$ 0.37	128.3 $\pm$ 11.5
2005 Nov 10.6	2453685.1	0.43	300 $\times$ 60	9.49 $\pm$ 0.13	1.25 $\pm$ 0.02	135.9 $\pm$ 0.4	2.44 $\pm$ 0.92	117.8 $\pm$ 20.6

<sup>a</sup> Orbital phase calculated for  $t_0 = \text{JD } 2\,443\,366.775$  and  $P=26.4960\text{days}$  (Gregory 2002). <sup>b</sup> Total exposure time is expressed as the integrated time per one frame, multiplied by the number of frames. <sup>c</sup> degree of observed polarization and it's position angle in the synthetic V-band (Bessel 1990; Kawabata et al. 1999). <sup>d</sup> Polarization of the H $\alpha$  line emission component. See §3.3.

**Table 2.** Observation of radio jet in the literature

Epoch	Array	$\Phi^h$	State	PA ( $^\circ$ )
1987 Sep 25 <sup>a</sup>		0.56	quiescent	
1987 Oct 1 <sup>a</sup>	EVN	0.79	burst(decaying)	
1990 Jun 6 <sup>b</sup>	EVN+VLA	0.71	burst(decaying)	$\sim 135, \sim 30$
1992 Jun 8 <sup>c</sup>	Global VLBA	0.39	quiescent(minioutburst)	$\sim 160$
1993 Sep 9 <sup>d</sup>	Global VLBA	0.66	burst(variable)	
1993 Sep 13 <sup>d</sup>		0.81	quiescent	$\sim 120$
1994 Jun 7 <sup>e</sup>	EVN	0.89	quiescent	$\sim 120$
1999 Sep 16-17 <sup>f</sup>	HALCA+Global VLBA	0.65	burst(variable)	
2001 Apr 22-23 <sup>g</sup>	MERLIN	0.68	quiescent	$\sim 124$
		0.71	preburst	$\sim 67$

<sup>a</sup>Taylor et al. 1992; <sup>b</sup>Massi et al. 1993; <sup>c</sup>Peracaula et al. 1998; <sup>d</sup>Paredes et al. 1998; <sup>e</sup>Massi et al. 2001; <sup>f</sup>Taylor et al. 2000; <sup>g</sup>Massi et al. 2004a; <sup>h</sup>Orbital phase is calculated in the same method of Table 1.

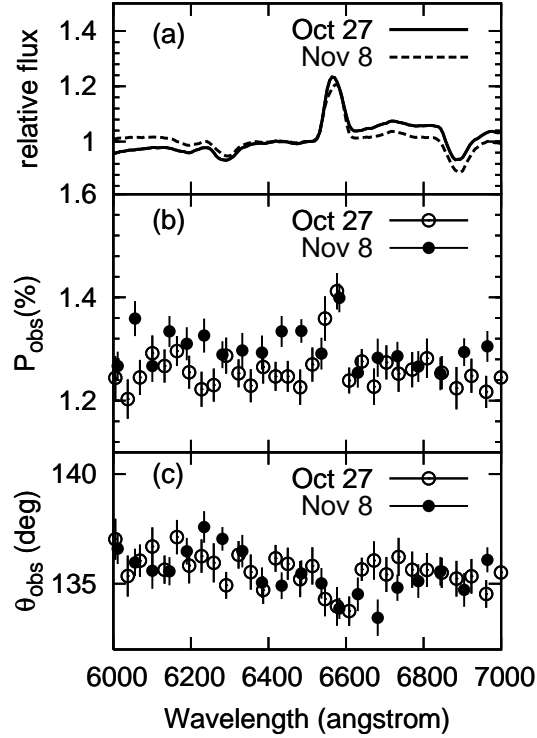


**Fig. 2.** Enlarged plot of Fig.1 around the H $\alpha$  line. From top to bottom, we plot (a) relative flux (flux at 6500 Å = 1), (b) degree of polarization and (c) its position angle. In (a) airmass effects are not calibrated, but the data are corrected for the instrumental response function. We can see a clear change of polarization across H $\alpha$  emission line, which suggests an existence of a polarization component intrinsic to the target star.

- Kaufman Bernadó, M. M., Romero, G. E., & Mirabel, I. F. 2002, A&A, 385, L10  
 Kanbach, G., Straubmeier, C., Spruit, H. C., & Belloni, T. 2001, Nature, 414, 180  
 Kawabata, K. S., et al. 1999, PASP, 111, 898  
 Lai, D., Chernoff, D.F., & Cordes, J.M., 2001, ApJ, 549, 1111  
 Lestrade, J.-F., Preston, R.A., Jones, D.L., Phillips, R.B., Rogers, A.E.E., Titus, M.A., Rioja, M.J., & Gabuzda, D.C. 1999, A&A, 344, 1014  
 Martí, J., & Paredes, J.M. 1995, A&A, 298, 151  
 Massey, P., Strobel, K., Barnes, J. V., & Anderson, E. 1988, ApJ, 328, 315  
 Massi, M., Paredes, J.M., Estalella, R., & Felli, M. 1993, A&A, 269, 249  
 Massi, M., Ribó, M., Paredes, J.M., Peracaula, M., & Estalella, R. 2001, A&A, 376, 217  
 Massi, M., Ribo, M., Paredes, J.M., Garrington, S.T., Peracaula, M., & Martí, J. 2004, A&A, 414, L1  
 Massi, M. 2004, A&A, 422, 267  
 McLean, I. S., & Clarke, D. 1979, MNRAS, 186, 245  
 Mirabel, I.F., & Rodrigues, L.F. 1999, ARA&A, 37, 409  
 Mirabel, I.F., Rodrigues, L.F., & Liu, Q.Z. 2004, A&A, 422, L29  
 Paredes, J.M., & Figueras, F. 1986, A&A, 154, L30

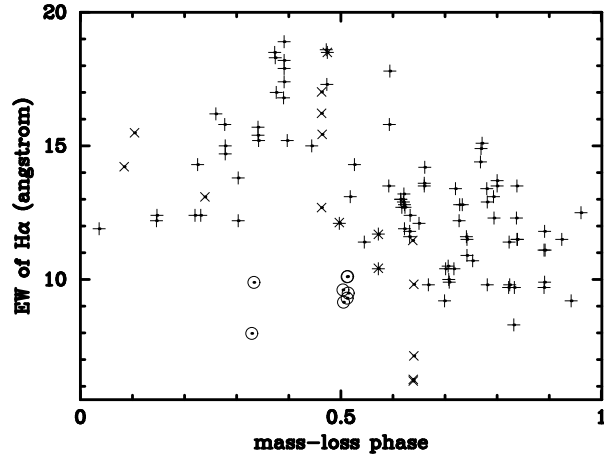


**Fig. 3.** Equivalent width of H $\alpha$  emission line as a function of the phase of mass-loss determined by radio flux (Gregory et al. 1999). Crosses are from Zamanov et al. (1999), inclined crosses are Paredes et al. (1994), and circle denote our results. Our results are commonly small compared with past observations.

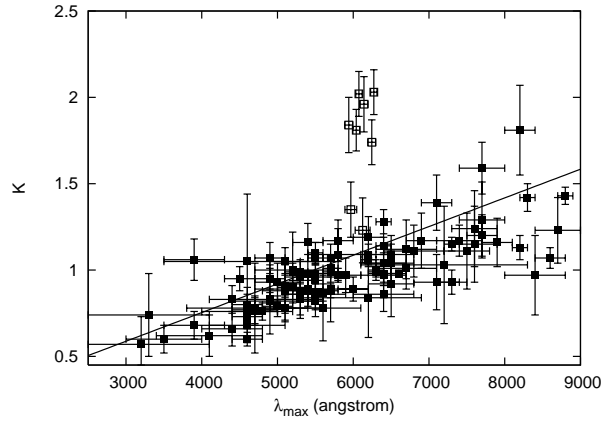


**Fig. 4.**  $K$  vs  $\lambda_{\max}$  derived for our nightly-averaged data (open square) are plotted together with samples of typical ISP (filled square). The sample stars are from Whittet et al. (1992). The solid line is  $K = 1.66\lambda_{\max} (\mu\text{m}) + 0.09$ , which well represents the correlation between  $K$  and  $\lambda_{\max}$  of ISP (Whittet et al. 1992). The  $K$  values of our data are commonly apart from the line (except for 2 data points, which would be affected by noise), which indicates that the observed polarization cannot be explained by only ISP.

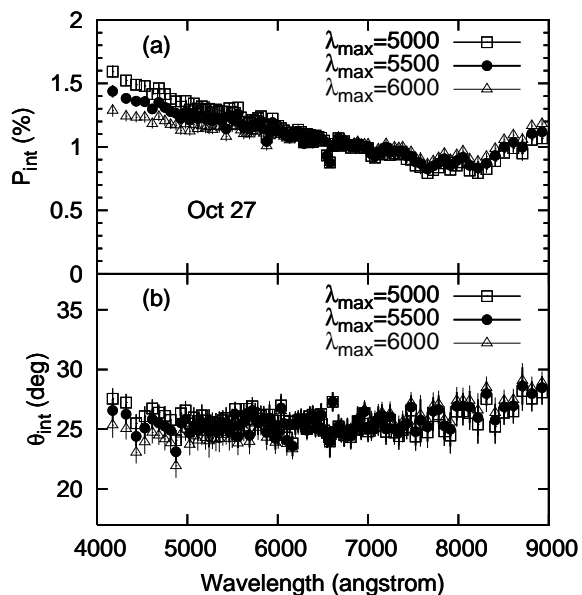


**Fig. 5.** Spectra of intrinsic polarization. (a) degree of the intrinsic polarization and (b) its position angle. The data are binned with the same manner in Figure 1. The wavelength dependence of polarization is quite similar to that of a typical Be star, e.g.,  $\zeta$  Tau (Wood et al. 1997). In a Be star, intrinsic polarization is originated by wavelength-independent Thomson scattering in the equatorial disk. The gradual decrease of polarization with wavelength from  $\sim 4000$  to  $\sim 8000$  Å and the polarization jump beyond 8000 Å are explained by unpolarized bound-free emission from hydrogen plasma.

- Paredes, J.M., Estalella R., & Rius, A. 1990, A&A, 232, 377  
Paredes, J.M., et al. 1994, A&A, 288, 519  
Paredes, J.M., Martí, J., Peracaula, M., & Ribó, M. 1997, A&A, 320, L25  
Paredes, J.M., Massi, M., Estalella, R., & Peracaula, M. 1998, A&A, 335, 539  
Paredes, J.M., Peracaula, M., Ribó, M., & Martí, J. 1999, Mem. Soc. Astron. Italiana, 70, 1139  
Paredes, J.M. 2005, CJAA Vol5, page121  
Peracaula, M., Gabuzda, D.C., & Taylor, A.R. 1998, A&A, 330, 612  
Poeckert, R. 1975, ApJ, 196, 777  
Poeckert, R., & Marlborough, J.M. 1977, ApJ, 218, 220  
Quirrenbach, A. et al. 1997, ApJ, 479, 477  
Ribó, M. 2005, ASPC, 340, 269R  
Romani, R.W. & Ng, C.-Y. 2003, ApJ, 585, 41  
Romero, G. E., Kaufman Bernadó, M. M., & Mirabel, I. F. 2002, A&A, 393, L61  
Scaltriti, F., Bodo, G., Ghisellini, G., Fiozzi, M., & Trussoni, E. 1997, A&A, 325, L29  
Serkowski, K., Mathewson, D.L., & Ford, V.L. 1975, ApJ, 196, 261  
Taylor A.R., & Gregory P.C. 1982, MNRAS, 360, 1105  
Taylor, B. J. 1984, ApJS, 54, 259  
Taylor A.R., Kenny, H.T., Spencer, R.E., & Tzioumis, A. 1992, ApJ, 395, 268  
Taylor, A. R., Dougherty, S. M., Scott, W. K., Peracaula, M., & Paredes, J. M. 2000, proc. of  
Astrophysical Phenomena Revealed by Space VLBI, ed. H. Hirabayashi, P.G. Edwards, & D.W.

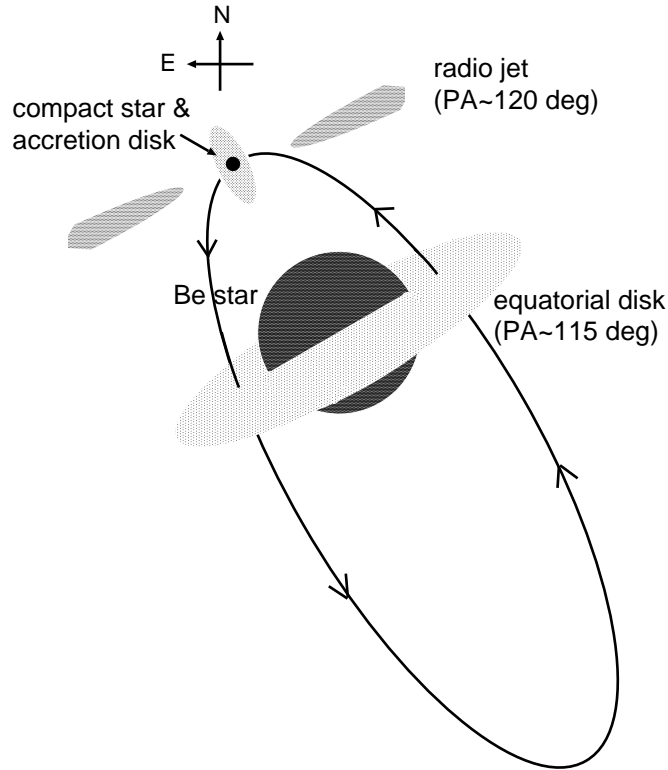


**Fig. 6.** Schematic representation of circumstellar geometry model of LS I +61° 303. The rotational axis of the Be star is nearly perpendicular to that of the accretion disk around the compact star. The compact star is likely to get across the equatorial disk of the Be star around its periastron passage (see figure 7).

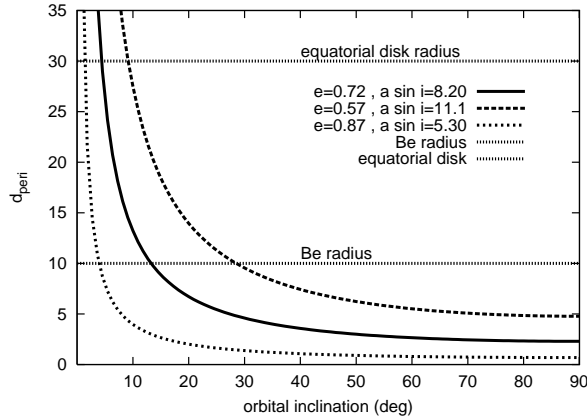


**Fig. 7.** Estimated binary separation at the periastron passage ( $d_{\text{peri}}$ ) as a function of orbital inclination  $i$ . For the calculation we used orbital parameters derived by Casares et al. (2005) with typical stellar parameters of a B0V star. The range of probable  $d_{\text{peri}}$  values lies between the two dashed curves. The compact star is likely to get across the equatorial disk of the Be star.



Murphy, 223

Uemura, M., et al. 2004, PASJ, 56, S61

Wang, N., Johnston, S., & Manchester, R.N. 2004, MNRAS, 351, 599

Waters, L.B.F.M., Taylor, A.R., van den Heuvel, E.P.J., Habets, G.M.H.J., & Persi, P. 1988, A&A, 198, 200

Wex, N., Johnston, S., Manchester, R.N., Lyne, A.G., Stappers, B.w., & Bailes, M. 1998, MNRAS, 298, 997

Whittet, D.C.B., Martin, P.G., Hough, J.H., Rouse, M.F., Bailey, J.A., & Axon, D.J. 1992, ApJ, 386, 562

Wolff, M. J., Nordsieck, K. H., & Nook, M. A. 1996, AJ, 111, 856

Wood, K., Bjorkman, K.S., & Bjorkman, J.E. 1997, ApJ, 477, 926

Zamanov, R.K., Martí, J., Paredes, J.M., Fabregat, J., Ribó, M., & Tarasov, A.F. 1999, A&A, 351, 543